

# RSC Advances



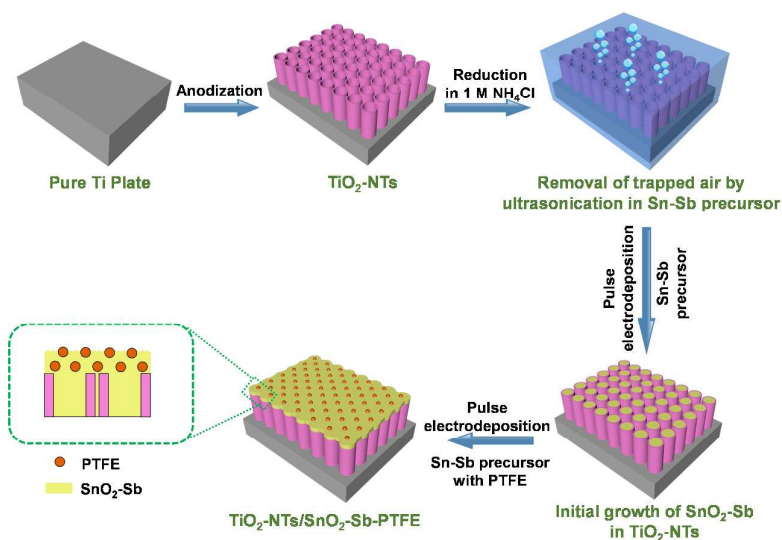
This is an *Accepted Manuscript*, which has been through the Royal Society of Chemistry peer review process and has been accepted for publication.

*Accepted Manuscripts* are published online shortly after acceptance, before technical editing, formatting and proof reading. Using this free service, authors can make their results available to the community, in citable form, before we publish the edited article. This *Accepted Manuscript* will be replaced by the edited, formatted and paginated article as soon as this is available.

You can find more information about *Accepted Manuscripts* in the [Information for Authors](#).

Please note that technical editing may introduce minor changes to the text and/or graphics, which may alter content. The journal's standard [Terms & Conditions](#) and the [Ethical guidelines](#) still apply. In no event shall the Royal Society of Chemistry be held responsible for any errors or omissions in this *Accepted Manuscript* or any consequences arising from the use of any information it contains.

## Table of contents



Novel TiO<sub>2</sub>-NTs/SnO<sub>2</sub>-Sb-PTFE electrodes were fabricated by pulse electrodeposition with higher oxygen evolution potential, improved surface hydrophobicity and enhanced electrocatalytic activity.

## ARTICLE

# Enhanced electrochemical oxidation of phenol using hydrophobic TiO<sub>2</sub>-NTs/SnO<sub>2</sub>-Sb-PTFE electrode prepared by pulse electrodeposition

Cite this: DOI: 10.1039/x0xx00000x

Weiyi Wu,<sup>a, b</sup> Zhao-Hong Huang<sup>c</sup> and Teik-Thye Lim<sup>a, b\*</sup>Received 00th January 2012,  
Accepted 00th January 2012

DOI: 10.1039/x0xx00000x

www.rsc.org/

In this study, novel Sb-doped SnO<sub>2</sub> electrodes with polytetrafluoroethylene (PTFE) composite were fabricated by pulse electrodeposition. In this process, vertically aligned TiO<sub>2</sub> nanotubes (TiO<sub>2</sub>-NTs) formed by anodization of Ti plate served as the substrate for SnO<sub>2</sub> electrodeposition. Comparing with the conventional SnO<sub>2</sub>-Sb electrodes, TiO<sub>2</sub>-NTs/SnO<sub>2</sub>-Sb-PTFE electrodes have higher oxygen evolution potential, improved surface hydrophobicity, superior hydroxyl radicals (HO<sup>•</sup>) generation and enhanced electrocatalytic activity by incorporation of PTFE nanoparticles. Field emission scanning electron microscopy (FESEM) shows that the surfaces of the PTFE composite electrodes exhibit microspherical structure. Energy-dispersive X-ray spectroscopy (EDS) confirms the uniform distribution of Sn, Sb, F and C on TiO<sub>2</sub>-NTs/SnO<sub>2</sub>-Sb-PTFE surfaces. More importantly, the electrodes exhibit a distinctive improvement of oxygen evolution potential (OEP) from 2.0 to 2.4 V (vs Ag/AgCl). The electrochemical impedance of TiO<sub>2</sub>-NTs/SnO<sub>2</sub>-Sb-PTFE also decreases significantly compared with Ti/SnO<sub>2</sub>-Sb(conventional). The electrocatalytic performance of TiO<sub>2</sub>-NTs/SnO<sub>2</sub>-Sb-PTFE compared with Ti/SnO<sub>2</sub>-Sb(conventional) and TiO<sub>2</sub>-NTs/SnO<sub>2</sub>-Sb were investigated using phenol as the model pollutant. The effects of initial solution pH and types of supporting electrolyte were investigated. The removal efficiency of total organic carbon (TOC), specific UV absorbance at 254 nm (SUVA<sub>254</sub>) mineralization current efficiency (MCE) and energy consumption (E<sub>c</sub>) with respect to different PTFE loadings on the electrodes were investigated. The anodic leaching of Sn ions was also studied in different conditions.

## 1. Introduction

For many years, the presence of biorefractory or recalcitrant compounds hinders the treatment of industrial wastewater. An alternative technology to conventional biological treatment methods is advanced oxidation processes (AOPs), which can remove or alleviate the refractory compounds by in situ generation of highly reactive oxygen species (ROS), mainly hydroxyl radicals (HO<sup>•</sup>). Among the AOPs, electrochemical oxidation has received special interest for the advantage of employing clean reagent electron for reaction, which has the environmental merit to minimize secondary pollutants.<sup>1</sup> From the viewpoint of environmental applications, it is critical to develop electrodes with good physical, chemical and electrochemical stability, high conductivity, high selectivity and satisfactory efficiency for organic oxidation.<sup>2-4</sup>

Recently, increasing efforts have been put forward to using mixed metal oxides (MMOs) as anode materials to remove various types of recalcitrant organic pollutants.<sup>5-8</sup> Among the MMOs, antimony doped SnO<sub>2</sub> (SnO<sub>2</sub>-Sb) has been demonstrated to be a very promising material with several advantages such as relatively high oxygen evolution overpotential, easy preparation, low cost and superior performance for the electrochemical oxidation of organic

compounds. Pollutants such as phenol and phenolic compounds can be readily oxidized at SnO<sub>2</sub>-Sb anode comparing with Pt and other MMO anodes, favoring complete oxidation of pollutants to CO<sub>2</sub> and H<sub>2</sub>O.<sup>9-11</sup> However, the short service life of SnO<sub>2</sub>-Sb electrode resulting from the weak adhesion between Ti substrate and SnO<sub>2</sub><sup>12,13</sup> or the formation of nonstoichiometry SnO<sub>(2-x)</sub><sup>14</sup> has represented an insurmountable barrier to its commercial applications.

Various attempts have been made to overcome this problem and improve the electrocatalytic performance of SnO<sub>2</sub>-Sb electrodes. One approach is to develop doped SnO<sub>2</sub>-Sb electrodes by including some noble or transition metal ions (Bi, Ir, Fe, Ni, Eu, La, Ce, Ru or Gd, etc.) into the precursor solutions or electrodeposition bath.<sup>15-24</sup> By introducing dopants improvement of the electrocatalytic performances of SnO<sub>2</sub>-Sb electrodes would be obtained. However, there are still some remarkable limitations of this approach. For example, the presence of Ce did not lead to higher removal of pollutant although the service lifetime was enhanced.<sup>22</sup> The incorporation of Eu reduced the grain sizes of SnO<sub>2</sub>-Sb but the increase of oxygen vacancies of SnO<sub>2</sub> was undesirable for its electrocatalytic performance.<sup>18</sup> Moreover, the introduction of Ir led to a lower oxygen evolution potential (OEP).<sup>23</sup> Therefore,

is important to develop highly stable SnO<sub>2</sub>-Sb electrode without sacrificing its electrocatalytic activity.

Recently, SnO<sub>2</sub> electrodes with nanostructured and microstructured design have drawn much interest. One of the most important approaches is by employing highly ordered substrate.<sup>10, 25, 26</sup> Highly ordered vertically aligned TiO<sub>2</sub> nanotubes (TiO<sub>2</sub>-NTs) can be prepared by anodization of Ti substrates, with mean pore diameters ranging from 100 to 220 nm. With the property of large surface area, TiO<sub>2</sub>-NTs can serve as tubular template wherein SnO<sub>2</sub>-Sb are implanted aiming to obtain improved loading capacity of Ti substrate.<sup>27</sup> TiO<sub>2</sub>-NTs/SnO<sub>2</sub>-Sb prepared by pulse electrodeposition has been verified to have distinctive oxygen evolution potential of about 2.4 V vs SCE and show remarkable better electrocatalytic activity compared with the SnO<sub>2</sub>-Sb electrode prepared by sol-gel method.<sup>28</sup> Meanwhile, polymers are attractive materials to introduce specific properties of metal oxide anodes. Polypyrrole and polytetrafluoroethylene (PTFE) composites have been used to introduce the hydrophobicity of PbO<sub>2</sub> electrode and obtained improved OEP and electrocatalytic activity.<sup>29, 30</sup> In other work, TiN composite has also been incorporated on SnO<sub>2</sub>-Sb electrode for improved electrocatalytic activity.<sup>31</sup>

In the present work, novel TiO<sub>2</sub>-NTs/SnO<sub>2</sub>-Sb-PTFE composite electrodes were fabricated by pulse electrodeposition for the first time to obtain the larger specific surface area and hydrophobic electrode surface. The surface morphology, crystalline structure and electrochemical properties of the novel electrodes were investigated. The capability of HO<sup>•</sup> generation on the electrodes were also evaluated. Phenol was selected as the model pollutant to investigate the performance of as-prepared electrodes. The effects of pH and supporting electrolytes (Na<sub>2</sub>SO<sub>4</sub> and NaCl) on the process efficiency were investigated, with a proposed mechanism presented to depict the electrochemical oxidation processes in different electrolytes. Sn ions leaching of TiO<sub>2</sub>-NTs/SnO<sub>2</sub>-Sb-PTFE was also studied under different conditions of electrochemical oxidation to evaluate its feasibility for environmental application.

## 2. Experimental

### 2.1 Chemicals and materials

All the chemicals were of analytical grade and used without further purification. SnCl<sub>2</sub>·2H<sub>2</sub>O, SbCl<sub>3</sub>, Na<sub>2</sub>SO<sub>4</sub>, NaCl, NaF, NH<sub>4</sub>Cl, PTFE, glycerol, dimethyl sulfoxide (DMSO), 2,4-dinitrophenylhydrazine and (3-aminopropyl)trimethoxysilane were obtained from Sigma-Aldrich. Merck's absolute acetone, NaOH pellet, HCl and phenol were used in the experiments. PTFE was in the form of emulsion with 60 wt % dispersion in water. Pure titanium plates (99.9%) with a thickness of 0.5 mm were purchased from Qixin Company (Baoji, China).

### 2.2 TiO<sub>2</sub>-NTs preparation

Pure titanium plates (60mm × 20mm) were polished by mechanical polisher with 120, 320, 800 and 1200 grid sand papers in sequence. Then they were washed in acetone and Milli Q water with ultrasonic assistance for 15 min, respectively. After that the titanium plates were immersed in 18% hydrochloric acid at 85 °C for 20 min to remove titanium oxide. In order to fabricate TiO<sub>2</sub>-NTs substrate, the clean Ti plate was anodized in a two-electrode cell (1 cm distance) at room

temperature, in which the clean Ti acted as anode and another titanium plate with same dimension as the cathode. The electrolyte is an aqueous solution containing a mixture of glycerol and Milli Q water (1.3:1 v/v), NaF (0.5 wt %) and Na<sub>2</sub>SO<sub>4</sub> (0.2 M). Anodization experiments were carried out at a voltage of 30 V for 240 min with continuous magnetic stirring. Finally, the prepared substrates were annealed at 500 °C for 90 min at both a heating and cooling rate of 1 °C min<sup>-1</sup> to get vertically aligned TiO<sub>2</sub>-NTs.

### 2.3 TiO<sub>2</sub>-NTs/SnO<sub>2</sub>-Sb-PTFE preparation

TiO<sub>2</sub>-NTs/SnO<sub>2</sub>-Sb-PTFE were prepared by pulse electrodeposition in a two-electrode cell (1 cm distance) using potentiostat (PGSTAT302N, Autolab) at 40 °C. Fig. 1 shows the schematic diagram for electrode design and preparation. Prior to pulse electrodeposition, TiO<sub>2</sub>-NTs were pretreated by reduction in 1 M NH<sub>4</sub>Cl at a potential of -1.5 V vs Ag/AgCl at 40 °C, aiming to improve the conductivity of TiO<sub>2</sub>-NTs substrate. Then the TiO<sub>2</sub>-NTs were vertically immersed into the electrolyte which was consisted of 0.1 M SnCl<sub>2</sub>·2H<sub>2</sub>O, 0.02 M SbCl<sub>3</sub> and a certain concentration of hydrochloric acid, and they were degassed in an ultrasonic bath for 10 min. This procedure was to remove the trapped air in the TiO<sub>2</sub>-NTs. The impregnation of NTs with electrolyte is expected to favor the initial growth of SnO<sub>2</sub>-Sb on the internal walls of the NTs. The nominal area of the electrode surface is 10 cm<sup>2</sup>.

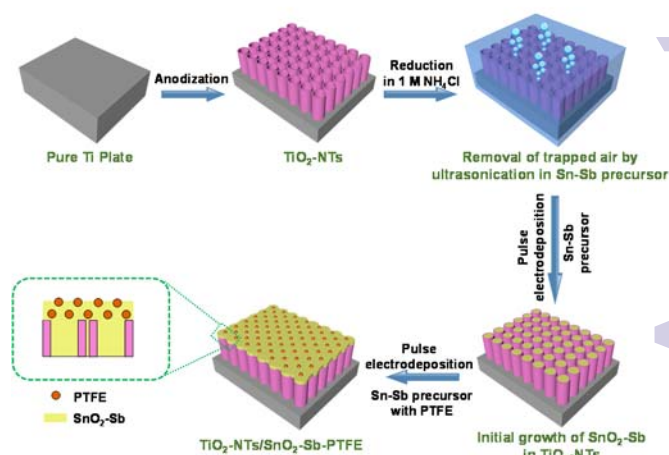


**Fig. 1** Schematic illustration of TiO<sub>2</sub>-NTs/SnO<sub>2</sub>-Sb-PTFE electrode preparation

The initial deposition of SnO<sub>2</sub>-Sb was conducted in the above electrolyte. A pulse current with an anodic pulse (5 mA cm<sup>-2</sup>, 50 ms), a cathodic pulse (-5 mA cm<sup>-2</sup>, 5 ms) and a relaxation time (0 mA cm<sup>-2</sup>, 1 s) was applied at 40 °C for 15 min. After that, the electrode was put into electrolytes consisted of 0.1 M SnCl<sub>2</sub>·2H<sub>2</sub>O, 0.02 M SbCl<sub>3</sub>, a certain concentration of hydrochloric acid and plural PTFE dispersions (0, 1.5, 4.5 and 13.5 mL L<sup>-1</sup>) using the same pulse electrodeposition method for 2 h. A 0.05 wt % (3-aminopropyl)trimethoxysilane solution was added in the electrolyte to lower the surface tension. The resulting electrodes were marked as TiO<sub>2</sub>-NTs/SnO<sub>2</sub>-Sb, TiO<sub>2</sub>-NTs/SnO<sub>2</sub>-Sb-PTFE(1.5), TiO<sub>2</sub>-NTs/SnO<sub>2</sub>-Sb-PTFE(4.5) and TiO<sub>2</sub>-NTs/SnO<sub>2</sub>-Sb-PTFE(13.5) with respect to the different concentrations of PTFE in the electrodeposition baths.

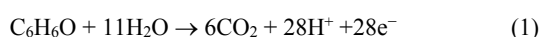
The conventional Ti/SnO<sub>2</sub>-Sb electrode having the same nominal surface area was prepared by thermochemical decomposition according to the literature.<sup>32</sup>

## 2.4 Bulk electrolysis experiments

Bulk electrochemical oxidation of phenol was carried out in a 200 ml single-compartment electrochemical cell at room temperature for 6 h under continuous stirring. Conventional Ti/SnO<sub>2</sub>-Sb electrode prepared by thermochemical decomposition, TiO<sub>2</sub>-NTs/SnO<sub>2</sub>-Sb and TiO<sub>2</sub>-NTS/SnO<sub>2</sub>-Sb-PTFE electrodes prepared by pulse electrodeposition were employed as the anodes, and a titanium plate with the same area served as the cathode. The distance between the two electrodes is 1 cm. The influencing factors that were investigated including the types of supporting electrolytes (Na<sub>2</sub>SO<sub>4</sub> and NaCl) and the initial solution pH (pH = 3, 7 and 11). Either 0.05 M Na<sub>2</sub>SO<sub>4</sub> or 0.1 M NaCl were used as the supporting electrolytes for synthetic wastewater solution containing 5 mM phenol. Initial pH of solutions were adjusted by adding drops of 1 M HCl, 0.5 M H<sub>2</sub>SO<sub>4</sub> or 1M NaOH solutions. The current density was set as 20 mA cm<sup>-2</sup>, and the samples were drawn for analysis with 1 h time interval. The accelerated life tests were conducted by anodic polarization at current density of 100 mA cm<sup>-2</sup> in 0.1 M H<sub>2</sub>SO<sub>4</sub> to evaluate the service lifetime of the electrodes. The accelerated life in hours was determined by the time when the cell potential increased 5 V from the initial value.<sup>32</sup>

The electrocatalytic performance of the electrodes were evaluated by measurement of total organic carbon (TOC) and specific ultraviolet absorbance at wavelength of 254 nm (SUVA<sub>254</sub>). SUVA<sub>254</sub> is defined as the UV absorbance at wavelength of 254 nm normalized by dissolved organic carbon (DOC) concentration, which is equivalent to the determined TOC since the solutions were crystal clear. The TOC of the samples were measured by a TOC analyzer (TOC-L/CPH, Shimadzu). The UV absorbance of the samples at wavelength of 254 nm were determined by a UV-Vis spectrophotometer (UV 9000, Metash). HO<sup>•</sup> was quantitatively determined by high-performance liquid chromatography (HPLC, Perkin Elmer Series 200) with DMSO trapping according to literature.<sup>33</sup> The organic acids intermediates of phenol oxidation were qualitatively determined by ion chromatography (IC, Thermo Scientific Dionex ICS-2100). Atomic absorption spectroscopy (AAS, Perkin Elmer AAnalyst 100) was used to analyze the leached Sn ions in the solutions after 6 h bulk electrolysis.

The completely electrochemical oxidation of phenol can be expressed as:



At given time *t*, the mineralization current efficiency (MCE) of the electrochemical oxidation process can be calculated by the following equation:<sup>34</sup>

$$\text{MCE (\%)} = \frac{100 \cdot \Delta[\text{TOC}]_{\text{exp}}}{\Delta[\text{TOC}]_{\text{theory}}} \quad (2)$$

where  $\Delta[\text{TOC}]_{\text{exp}}$  and  $\Delta[\text{TOC}]_{\text{theory}}$  (mg dm<sup>-3</sup>) are the experimental TOC change and theoretical TOC change at given time *t*, respectively. The value of  $\Delta(\text{TOC})_{\text{theory}}$  can be calculated by:

$$\Delta[\text{TOC}]_{\text{theory}} = \frac{1000 \cdot n_c \cdot I t M}{n_e F V} \quad (3)$$

where *n<sub>c</sub>* is the number of organic carbon, *I* is the applied current (A), *t* is the electrolysis time (s), *M* is the atomic weight of carbon (*M* = 12 g mol<sup>-1</sup>), *n<sub>e</sub>* is the number of electron transfers, *F* is the Faradic constant (96485 C mol<sup>-1</sup>) and *V* is the volume of solution (dm<sup>3</sup>). For phenol oxidation, *n<sub>c</sub>* and *n<sub>e</sub>* are 28 and 6 respectively.

The specific energy consumption (*E<sub>c</sub>*, kWh kgTOC<sup>-1</sup>) can be calculated as follows:

$$E_c = \frac{1000 \cdot E_{\text{cell}} \cdot I t}{\Delta[\text{TOC}]_{\text{exp}} V} \quad (4)$$

where *E<sub>cell</sub>* is the average cell potential (V), *I* is the applied current (A), *t* is the electrolysis time (h),  $\Delta[\text{TOC}]_{\text{exp}}$  is the experimental TOC change (mg dm<sup>-3</sup>) and *V* is the volume of solution (dm<sup>3</sup>).

## 2.5 Analytical techniques

The surface morphology and element composition of the electrodes were characterized using field emission scanning electron microscopy (FESEM, JEOL-7660F) and energy dispersive X-ray spectroscopy (EDS, Oxford Xmax80 LN2 Free). The crystal structure of the fabricated electrodes were characterized by X-ray diffraction (XRD, Bruker D8 Advance) with Cu-Kα ( $\lambda=1.5418 \text{ \AA}$ ) operating at 40 kV and 40 mA, with corresponding 2θ range of 10-80°. The contact angle of water on the electrode surface was determined by a contact angle meter (DSA100). Electrochemical properties of the electrodes were investigated in a conventional three-electrode system using electrochemical workstation (PGSTAT 302N, Autolab). Pt served as the counter electrode and Ag/AgCl served as the reference electrode, and the electrolyte was 0.5 M Na<sub>2</sub>SO<sub>4</sub>. Cyclic voltammetry (CV) was performed to determine the OEP of the electrode with the scan range of 0.3-3.0 V and scan rate of 50 mV s<sup>-1</sup>. Anodic polarization experiments were studied using chronoamperometric method at a potential of 1.4 V and 3.0 V vs Ag/AgCl respectively for 10 s with/without 5 mM phenol. Electrochemical impedance spectroscopy (EIS) was carried out at 1.0 V to measure the impedance of the electrodes. The frequency ranges from 100 kHz to 5 mHz with an amplitude of 10 mV, and equivalent circuit simulation was applied to determine the values of electrochemical parameters.

## 3. Results and discussion

### 3.1 Characteristics of TiO<sub>2</sub>-NTS/SnO<sub>2</sub>-Sb-PTFE

**3.1.1 Surface structure and wetting property.** The surface morphology of the TiO<sub>2</sub>-NTs substrate and the fabricated electrodes are examined by FESEM. As can be seen in Fig. 2a, highly ordered TiO<sub>2</sub>-NTs were uniformly grown on Ti plate with an average pore diameter of 100 nm, and the thickness of the wall ranges from 10 to 20 nm. The surface of the conventional SnO<sub>2</sub>-Sb electrodes shows "mud-cracked" structure (Fig. 2b), which is a typical structure in MMO anodes prepared by thermochemical decomposition. The cracks is undesirable because it would give rise to the weak adhesion between SnO<sub>2</sub> and Ti substrate. In addition, such cracks may lead to the permeation of electrolyte into the Ti substrate, and finally the formation of a passivating layer between SnO<sub>2</sub>-Sb and Ti substrate. It was also confirmed by the accelerated life test that the conventional Ti/SnO<sub>2</sub>-Sb electrode has a lowest service lifetime of only 6.4 h (Table 1). In Fig. 2c, improvement of the surface morphology is observed in TiO<sub>2</sub>-

NTs/SnO<sub>2</sub>-Sb fabricated by pulse electrodeposition. The SnO<sub>2</sub>-Sb nanoparticles show microspherical shape with diameters ranging from 100 to 200 nm, and no crack is observed on the electrode surface comparing with the conventional Ti/SnO<sub>2</sub>-Sb. The service lifetime of TiO<sub>2</sub>-NTs/SnO<sub>2</sub>-Sb was also improved up to 28h, which is 4.3 times that of the conventional Ti/SnO<sub>2</sub>-Sb. After the incorporation of PTFE nano particles, a layer of PTFE can be observed on the surfaces of all the three electrodes with different PTFE loadings (Fig. 2d-f). Compared with TiO<sub>2</sub>-NTs/SnO<sub>2</sub>-Sb without PTFE, the electrode surfaces with PTFE loading become rough in morphology. Such morphology leads to increased specific surface area which can provide more active sites for the electrocatalytic oxidation reactions to take place. It is also notable that a reduced SnO<sub>2</sub>-Sb particle grain size is observed at TiO<sub>2</sub>-NTs/SnO<sub>2</sub>-Sb-PTFE(4.5), indicating grain refining effect for SnO<sub>2</sub>-Sb deposition. The accelerated service lifetime of TiO<sub>2</sub>-NTs/SnO<sub>2</sub>-Sb-PTFE(4.5) and TiO<sub>2</sub>-NTs/SnO<sub>2</sub>-Sb-PTFE(13.5) were further improved up to 98h and 103 h, corresponding to 15.3 and 16 times that of the conventional SnO<sub>2</sub>-Sb, respectively.

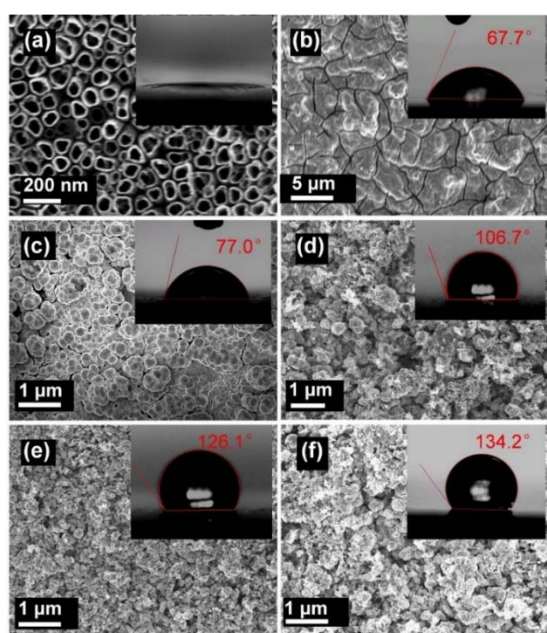


**Fig. 2** FESEM images and contact angles (inset) of (a) TiO<sub>2</sub>-NTs, (b) conventional TiO<sub>2</sub> /SnO<sub>2</sub>-Sb, (c) TiO<sub>2</sub>-NTs/SnO<sub>2</sub>-Sb, (d) TiO<sub>2</sub>-NTs/SnO<sub>2</sub>-Sb-PTFE(1.5), (e) TiO<sub>2</sub>-NTs/SnO<sub>2</sub>-Sb-PTFE(4.5) and (f) TiO<sub>2</sub>-NTs/SnO<sub>2</sub>-Sb-PTFE(13.5)

Elements of Ti, Sn, Sb, F, C and O were detected by EDS on TiO<sub>2</sub>-NTs/SnO<sub>2</sub>-Sb-PTFE electrodes. Fig. 3 shows the uniform distribution of elements Sn, Sb, F and C on TiO<sub>2</sub>-NTs/SnO<sub>2</sub>-Sb-

PTFE(4.5) by elemental mapping. The atomic percentages of the elements are investigated and listed in Table 2. There is still a small portion of Ti detected on the electrode surfaces. However, more amount of Ti was detected on the conventional Ti/SnO<sub>2</sub>-Sb (1.15%), which is possibly due to the cracks of the electrode leading to the exposure of Ti substrate. Sb/Sn ratios of TiO<sub>2</sub>-NTs/SnO<sub>2</sub>-Sb-PTFE electrodes are around 4%, while the value is 2.6% on the conventional Ti/SnO<sub>2</sub>-Sb. It should be noted that when the PTFE loading in the electrodeposition bath increases 3 times from 4.5 ml L<sup>-1</sup> to 13.5 ml L<sup>-1</sup>, the real atomic percentage of F in the electrode surface only increases by a factor of 1.8 (from 0.58% to 1.08%). It indicates that PTFE loading of TiO<sub>2</sub>-NTs/SnO<sub>2</sub>-Sb-PTFE(13.5) has reached a saturation level and further increase of PTFE in the electrodeposition bath would not result in higher PTFE content in the electrode surface.

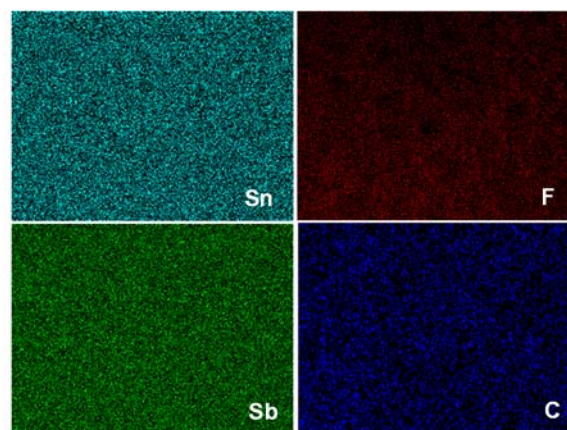


**Fig. 3** Elemental mappings of Sn, Sb, F and C on the surface of TiO<sub>2</sub>-NTs/SnO<sub>2</sub>-Sb-PTFE(4.5)

The contact angle of TiO<sub>2</sub>-NTs (Fig. 2a) is very low (below 10°) and shows its super hydrophilic property. Both the conventional Ti/SnO<sub>2</sub>-Sb and TiO<sub>2</sub>-NTs/SnO<sub>2</sub>-Sb have hydrophilic surface (contact angles 67.7° and 77° respectively). For TiO<sub>2</sub>-NTs/SnO<sub>2</sub>-Sb-PTFE, because of the strong hydrophobicity of PTFE, its surface wetting property prominently changes and the contact angles are 106.7°, 126.7° and 134.2° respectively with the increasing PTFE loading.

Fig. 4 compares the XRD patterns of various electrodes. TiO<sub>2</sub> is indexed to anatase phase with diffraction peaks at 2θ = 25.6°, 38.1° and 48.3°. The diffraction peaks at 2θ = 26.8°, 34.1° and 52.0° are indexed to the (110), (101) and (211) planes of SnO<sub>2</sub>. No obvious peaks of Sb are detected due to the incorporation of Sb into the SnO<sub>2</sub> crystals. The intensities of (101) and (211) peaks for SnO<sub>2</sub> of conventional Ti/SnO<sub>2</sub>-Sb

**Table 1** Parameters of the Ti/SnO<sub>2</sub>-Sb(conventional), TiO<sub>2</sub>-NTs/SnO<sub>2</sub>-Sb and TiO<sub>2</sub>-NTs/SnO<sub>2</sub>-Sb-PTFE electrodes

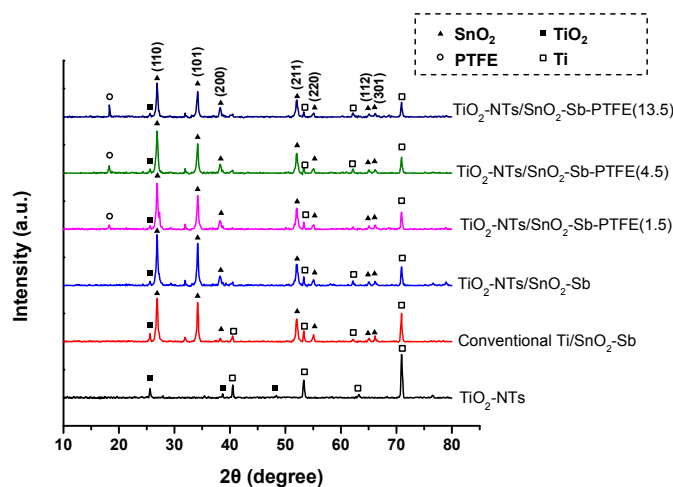
Electrode	OEP (V vs Ag/AgCl)	Service lifetime (h)	Current density without phenol <sup>a</sup> (mA cm <sup>-2</sup> )	Current density with phenol <sup>a</sup> (mA cm <sup>-2</sup> )	ΔCurrent density (mA cm <sup>-2</sup> )	Contact angle (°)
Conventional Ti/SnO <sub>2</sub> -Sb	2.0	6.4	8.32	10.54	2.22	67.7
TiO <sub>2</sub> -NTs/SnO <sub>2</sub> -Sb	2.1	28	8.47	11.60	3.13	77.0
TiO <sub>2</sub> -NTs/SnO <sub>2</sub> -Sb-PTFE(1.5)	2.2	51	10.29	14.71	4.42	106.7
TiO <sub>2</sub> -NTs/SnO <sub>2</sub> -Sb-PTFE(4.5)	2.4	98	10.21	16.55	6.34	126.1
TiO <sub>2</sub> -NTs/SnO <sub>2</sub> -Sb-PTFE(13.5)	2.4	103	9.36	12.41	3.05	134.2

<sup>a</sup> Current densities were measured at the potential of 3.0 V vs Ag/AgCl.

**Table 2** Elemental compositions of Ti/SnO<sub>2</sub>-Sb(conventional), TiO<sub>2</sub>-NTs/SnO<sub>2</sub>-Sb and TiO<sub>2</sub>-NTs/SnO<sub>2</sub>-Sb-PTFE electrode surfaces

Electrode	Surface elemental composition (Atomic %)					
	Ti	Sn	Sb	C	F	O
Conventional Ti/SnO <sub>2</sub> -Sb	1.15	32.3	0.84	-	-	66.7
TiO <sub>2</sub> -NTs/SnO <sub>2</sub> -Sb	0.76	32.1	1.33	-	-	65.8
TiO <sub>2</sub> -NTs/SnO <sub>2</sub> -Sb-PTFE(1.5)	0.61	33.3	1.28	0.12	0.22	64.5
TiO <sub>2</sub> -NTs/SnO <sub>2</sub> -Sb-PTFE(4.5)	0.52	32.3	1.41	0.30	0.58	64.9
TiO <sub>2</sub> -NTs/SnO <sub>2</sub> -Sb-PTFE(13.5)	0.48	32.4	1.22	0.57	1.08	64.3

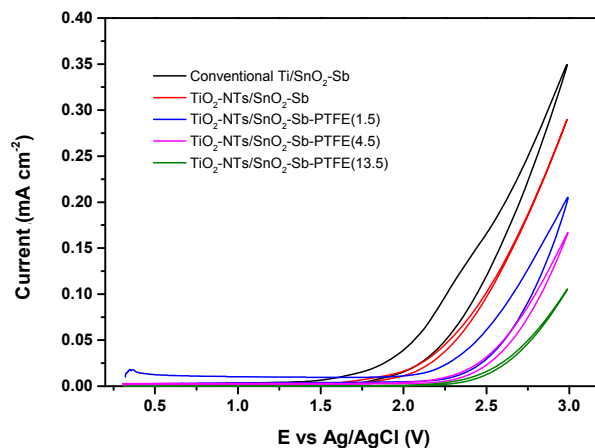
and TiO<sub>2</sub>-NTs/SnO<sub>2</sub>-Sb are similar. However, the intensity of (110) peak is much stronger in the conventional TiO<sub>2</sub>-NTs/SnO<sub>2</sub>-Sb, indicating a preferred orientation of SnO<sub>2</sub> along (110) direction. The diffraction peak at  $2\theta = 18.2^\circ$  suggests that PTFE has been successfully incorporated in the electrode surface coating. The higher PTFE loading, the stronger the peak intensity.

**Fig. 4** XRD patterns of the electrodes

**3.1.2 Electrochemical properties.** In environmental application of anodes, OEP is an important indicator of electrocatalytic activities for organics oxidation. Fig. 5 shows the CV curves of the conventional Ti/SnO<sub>2</sub>-Sb, TiO<sub>2</sub>-NTs/SnO<sub>2</sub>-Sb and TiO<sub>2</sub>-NTs/SnO<sub>2</sub>-Sb-PTFE electrodes in 0.5 M Na<sub>2</sub>SO<sub>4</sub>, and the corresponding values of OEP are given in Table 1. The conventional Ti/SnO<sub>2</sub>-Sb has a lowest OEP of 2.0 V, and the value increases slightly to 2.1 V in TiO<sub>2</sub>-NTs/SnO<sub>2</sub>-Sb fabricated by pulse electrodeposition. However, after introducing PTFE the OEP of the anodes are further increased, with the highest OEP of 2.4 V observed in TiO<sub>2</sub>-NTs/SnO<sub>2</sub>-Sb-PTFE(4.5) and TiO<sub>2</sub>-NTs/SnO<sub>2</sub>-Sb-PTFE(13.5). First, the enhancement of OEP is attributed to the change of surface wetting property from hydrophilic to hydrophobic, which inhibits the surface adsorption of hydrophilic HO<sup>•</sup>. Second, PTFE hinders the movement of HO<sup>•</sup> into the electrode interior. Thus, the oxygen evolution reaction (OER) is inhibited.<sup>30</sup>

The anodic polarization of the electrodes was studied at a constant potential of 1.4 V and 3.0 V vs Ag/AgCl to investigate their electrocatalytic activities towards phenol. At 1.4 V which is below the OEP, no background current was observed either in the presence or absence of phenol, suggesting phenol cannot be oxidized at this potential. When the potential was set as 3.0 V, the current densities of the five electrodes ranged from 8.32 mA cm<sup>-2</sup> to 10.29 mA cm<sup>-2</sup> in 0.5 M Na<sub>2</sub>SO<sub>4</sub> (Table 1). However, after the addition of 5 mM

phenol, there were drastic increases of the current densities. The increment of current density of TiO<sub>2</sub>-NTs/SnO<sub>2</sub>-Sb-PTFE(4.5) (6.34 mA cm<sup>-2</sup>) was significantly greater than that of conventional Ti/SnO<sub>2</sub>-Sb (2.22 mA cm<sup>-2</sup>) and TiO<sub>2</sub>-NTs/SnO<sub>2</sub>-Sb (3.13 mA cm<sup>-2</sup>) revealing its superior electrocatalytic activity towards phenol. Nevertheless, the value was much smaller in TiO<sub>2</sub>-NTs/SnO<sub>2</sub>-Sb-PTFE(13.5) (3.05 mA cm<sup>-2</sup>) compared with TiO<sub>2</sub>-NTs/SnO<sub>2</sub>-Sb-PTFE(4.5). Such phenomenon is attributed to their differences of surface morphology. The particle size of SnO<sub>2</sub>-Sb on TiO<sub>2</sub>-NTs/SnO<sub>2</sub>-Sb-PTFE(4.5) is much smaller, indicating more active sites for the oxidation of phenol to take place, so that the electrocatalytic activity is improved.

**Fig. 5** Cyclic voltammetric curves of the electrodes in 0.5 M Na<sub>2</sub>SO<sub>4</sub> with potential range of 0.3-3.0 V vs Ag/AgCl and scan rate of 50 mV s<sup>-1</sup>

EIS studies were carried out to further investigate the electrochemical impedance of the novel electrodes. Fig. 6a shows the Nyquist plots of the electrodes. As shown in the figure, well developed semicircle patterns are observed, which suggested that mass diffusion control is negligible.<sup>21</sup> TiO<sub>2</sub>-NTs substrate is non-conductive with an electrochemical impedance larger than 20000 Ω. After partial reduction of TiO<sub>2</sub>-NTs substrate and pulse electrodeposition of SnO<sub>2</sub>-Sb, the electrochemical impedance decreased significantly. Equivalent circuit module R<sub>s</sub>(R<sub>ct</sub>Q) was employed to better interpret the EIS results (Fig. 6b). The simulation values of the electrochemical parameters are given in Table 3. In this circuit model, R<sub>s</sub> represents the uncompensated ohmic resistance between the working electrode and reference electrode, R<sub>ct</sub> the charge transfer resistance, and Q is the constant phase element (CPE) of double layer. The values of n are all in the range of 0.75-1 representing the performance of the electrodes are close to pure capacitors. Comparing with the conventional Ti/SnO<sub>2</sub>-Sb, R<sub>s</sub> of TiO<sub>2</sub>-NTs/SnO<sub>2</sub>-Sb decreases by the

employment of TiO<sub>2</sub>-NTs substrate, suggesting better conductivity. Slight increases of R<sub>s</sub> are observed at TiO<sub>2</sub>-NTs/SnO<sub>2</sub>-Sb-PTFE electrodes. This is probably due to the property of PTFE which is non-conductive. Despite the slight increases of R<sub>s</sub>, it should be noted that the charge transfer resistances decrease significantly at TiO<sub>2</sub>-NTs/SnO<sub>2</sub>-Sb-PTFE electrodes. TiO<sub>2</sub>-NTs/SnO<sub>2</sub>-Sb-PTFE(4.5) has a lowest R<sub>ct</sub> of only 54.13 Ω cm<sup>-2</sup>, which is only 38% and 53% that of conventional Ti/SnO<sub>2</sub>-Sb and TiO<sub>2</sub>-NTs/SnO<sub>2</sub>-Sb by pulse electrodeposition. Lower R<sub>ct</sub> results in the faster electron transfer on electrode surface, indicating an improvement of electrocatalytic activity by incorporation of PTFE nanoparticles. Meanwhile, the R<sub>s</sub> of TiO<sub>2</sub>-NTs/SnO<sub>2</sub>-Sb-PTFE(4.5) (5.30 Ω cm<sup>-2</sup>) is also smaller than that of the conventional Ti/SnO<sub>2</sub>-Sb (5.89 Ω cm<sup>-2</sup>). Thus, TiO<sub>2</sub>-NTs/SnO<sub>2</sub>-Sb-PTFE(4.5) is expected to exhibit much better electrocatalytic activity. Moreover, the TiO<sub>2</sub>-NTs/SnO<sub>2</sub>-Sb-PTFE electrodes showed higher capacitance, which can result from electrochemically active surface area of the coatings.<sup>35</sup>

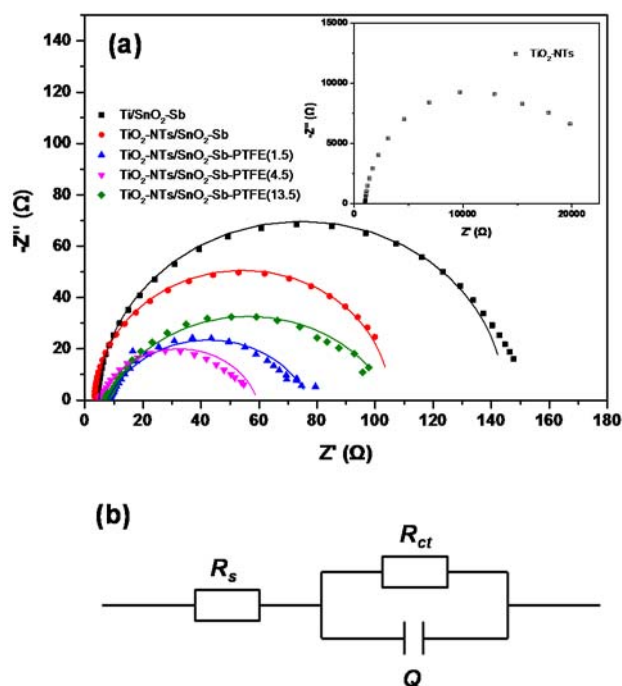


**Fig. 6** (a) Nyquist plots of the electrodes and simulation curves of the EIS results (inset is the Nyquist plot of TiO<sub>2</sub>-NTs) and (b) equivalent circuit model R<sub>s</sub>(R<sub>ct</sub>Q)

### 3.2 Electrochemical oxidation of phenol

**3.2.1 Influence of PTFE loadings.** Fig. 7 shows the removal of TOC during electrochemical oxidation of phenol in 0.05 M Na<sub>2</sub>SO<sub>4</sub>.

When using the conventional Ti/SnO<sub>2</sub>-Sb, the removal of TOC of phenol is only 69% after 6 h electrochemical oxidation at pH 7. An improvement of TOC removal (73%) is observed at TiO<sub>2</sub>-NTs/SnO<sub>2</sub>-Sb fabricated by pulse electrodeposition. As mentioned above, such enhancement is probably attributed to the reduced electrochemical impedance and the improved surface morphology of the 3-dimensional TiO<sub>2</sub>-NTs. Moreover, the TOC removal efficiency was greatly enhanced in TiO<sub>2</sub>-NTs/SnO<sub>2</sub>-Sb-PTFE electrodes (up to 93%), indicating the improved electrocatalytic activity of phenol oxidation by incorporation of PTFE in the electrode surfaces. The enhancement of TOC removal can be attributed to several reasons. First, the high OEP of TiO<sub>2</sub>-NTs/SnO<sub>2</sub>-Sb-PTFE favors the HO<sup>•</sup> generation. Second, the surfaces of TiO<sub>2</sub>-NTs/SnO<sub>2</sub>-Sb-PTFE electrodes are hydrophobic, so that the HO<sup>•</sup> generated would be released as free HO<sup>•</sup> rather than combining together for oxygen evolution. Hence, the removal efficiency is enhanced. The above results were verified by the HO<sup>•</sup> concentration in solution (Fig. 8). The TiO<sub>2</sub>-NTs/SnO<sub>2</sub>-Sb-PTFE electrodes showed superior ability of HO<sup>•</sup> generation (up to 36 μM) than Ti/SnO<sub>2</sub>-Sb (conventional) (26 μM) and TiO<sub>2</sub>-NTs/SnO<sub>2</sub>-Sb (28 μM) after 240 min bulk electrolysis. The best TOC removal was obtained in TiO<sub>2</sub>-NTs/SnO<sub>2</sub>-Sb-PTFE(4.5) which has the highest HO<sup>•</sup> generation (Fig. 7b). In addition, the TiO<sub>2</sub>-NTs/SnO<sub>2</sub>-Sb-PTFE(4.5) has notably smaller SnO<sub>2</sub>-Sb particles, which also give more active sites for phenol degradation.

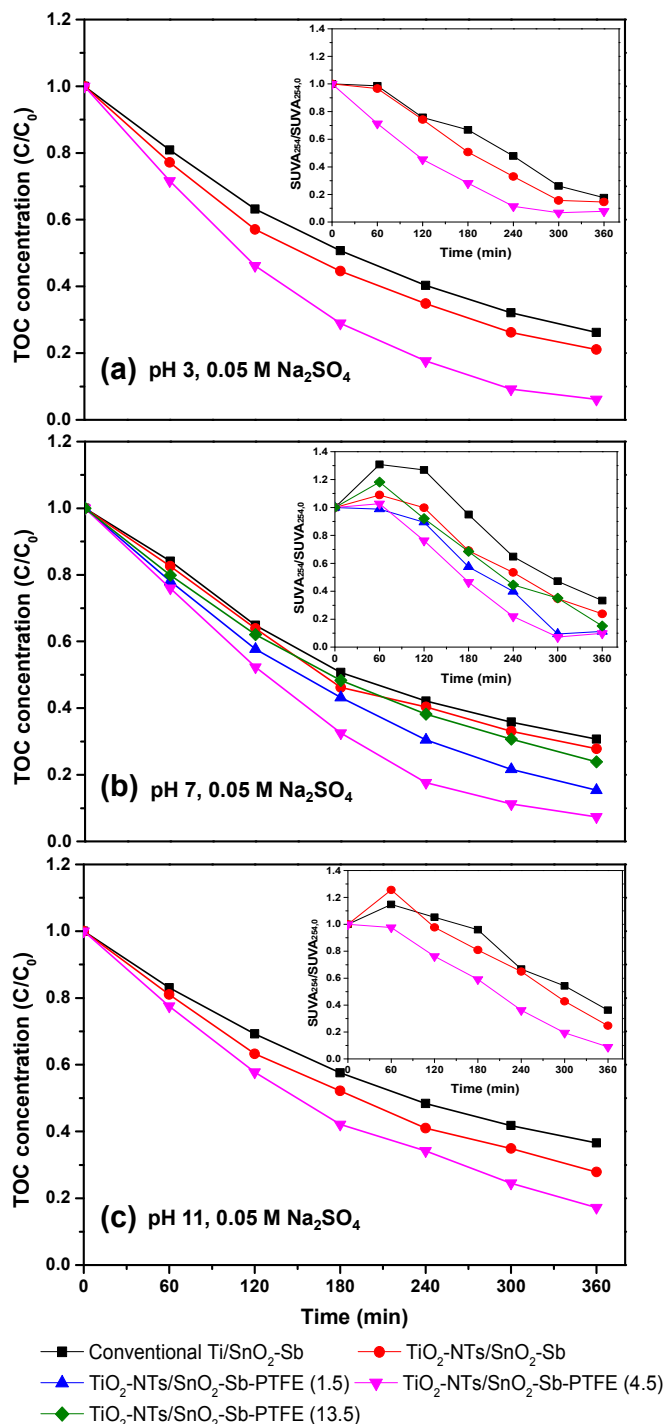
The SUVA<sub>254</sub> degradation of the 5 electrodes is represented in the inset of Fig. 7. SUVA<sub>254</sub> is strongly correlated with the aromatic extent of pollutants. The higher the SUVA<sub>254</sub>, the higher degree of aromaticity of the dissolved organic compounds.<sup>36</sup> Increase of SUVA<sub>254</sub> in the first hour using Ti/SnO<sub>2</sub>-Sb (conventional), TiO<sub>2</sub>-NTs/SnO<sub>2</sub>-Sb and TiO<sub>2</sub>-NTs/SnO<sub>2</sub>-Sb-PTFE(13.5) as anodes shows that the cleavage reaction of aromatic ring is not favored despite the TOC decreases. The main aromatic intermediates of phenol involves catechol, hydroquinone and benzoquinone.<sup>37</sup> When using TiO<sub>2</sub>-NTs/SnO<sub>2</sub>-Sb-PTFE(4.5) and TiO<sub>2</sub>-NTs/SnO<sub>2</sub>-Sb-PTFE(1.5) as anodes, the SUVA<sub>254</sub> decreased readily during the 6 h electrochemical oxidation, indicating phenol and aromatic intermediates undergo ring cleavage reactions. IC measurements showed that they were subsequently oxidized to aliphatic acids including maleic acid, oxalic acid, acetic acid and formic acid. Finally, they can be completely degraded to CO<sub>2</sub> and H<sub>2</sub>O. The final SUVA<sub>254</sub> after 6 h electrochemical oxidation is 0.098 SUVA<sub>254,0</sub> on TiO<sub>2</sub>-NTs/SnO<sub>2</sub>-Sb-PTFE(4.5), which is only 29% and 46% that of Ti/SnO<sub>2</sub>-Sb (conventional) and TiO<sub>2</sub>-NTs/SnO<sub>2</sub>-Sb. This result suggests that TiO<sub>2</sub>-NTs/SnO<sub>2</sub>-Sb-PTFE(4.5) has the merit of fully alleviating the aromatic intermediates into mineral acids, which are biodegradable and environmentally more benign.

Fig. 9a shows the MCE of different electrodes for electrocatalytic oxidation of phenol. The highest MCE was obtained on TiO<sub>2</sub>-NTs/SnO<sub>2</sub>-Sb-PTFE(4.5) (17.8 % at 1 h and 11.6 % at 6 h). Therefore, TiO<sub>2</sub>-NTs/SnO<sub>2</sub>-Sb-PTFE(4.5) exhibits the highest efficiency for electrocatalytic oxidation of

**Table 3** EIS simulating parameters of Ti/SnO<sub>2</sub>-Sb (conventional), TiO<sub>2</sub>-NTs/SnO<sub>2</sub>-Sb and TiO<sub>2</sub>-NTs/SnO<sub>2</sub>-Sb-PTFE electrodes

Electrodes	R <sub>s</sub> (error%) (Ω cm <sup>-2</sup> )	R <sub>ct</sub> (error%) (Ω cm <sup>-2</sup> )	n	CPE (error%) (mF cm <sup>-2</sup> )
Conventional Ti/SnO <sub>2</sub> -Sb	5.89 (0.48)	139.57 (0.74)	0.923	0.54 (0.59)
TiO <sub>2</sub> -NTs/SnO <sub>2</sub> -Sb	4.32 (1.26)	101.45 (0.633)	0.941	0.52 (1.12)
TiO <sub>2</sub> -NTs/SnO <sub>2</sub> -Sb-PTFE(1.5)	7.71 (3.41)	69.64 (6.44)	0.757	1.96 (16.47)
TiO <sub>2</sub> -NTs/SnO <sub>2</sub> -Sb-PTFE(4.5)	5.30 (2.31)	54.13 (3.77)	0.814	1.04 (11.90)
TiO <sub>2</sub> -NTs/SnO <sub>2</sub> -Sb-PTFE(13.5)	6.97 (2.32)	98.62 (5.49)	0.746	2.14 (9.74)

phenol. As shown in Fig. 9b,  $\text{TiO}_2\text{-NTs/SnO}_2\text{-Sb-PTFE}(4.5)$  has the lowest  $E_c$  among the 5 electrodes. The  $E_c$  of  $\text{TiO}_2\text{-NTs/SnO}_2\text{-Sb-PTFE}(4.5)$  to reach 60 % TOC removal is 49  $\text{kWh kgTOC}^{-1}$ , which is only 0.68 time that of  $\text{Ti/SnO}_2\text{-Sb}(\text{conventional})$  and 0.78 time that of  $\text{TiO}_2\text{-NTs/SnO}_2\text{-Sb}$ . On the basis of above analysis,  $\text{TiO}_2\text{-NTs/SnO}_2\text{-Sb-PTFE}(4.5)$  appears to be the most optimal electrode with the most TOC removal and  $\text{SUVA}_{254}$  decrease, highest MCE and lowest energy consumption.



**Fig. 7** TOC concentration and  $\text{SUVA}_{254}$  as a function of time during phenol degradation at: (a) pH 3; (b) pH 7; (c) pH 11

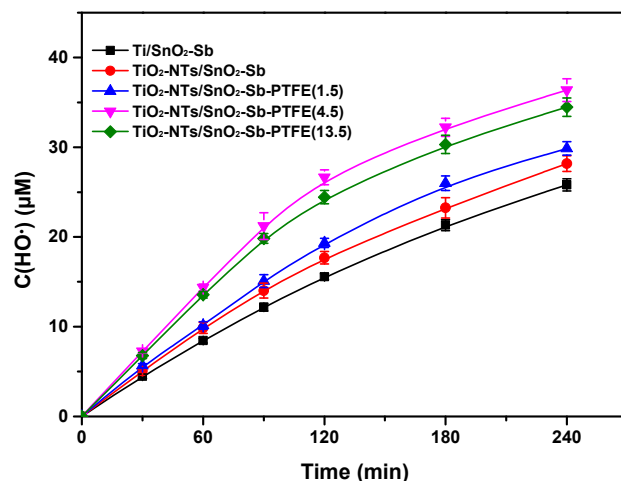


**Fig. 8** Concentration evolution of hydroxyl radicals on the electrodes in  $0.05 \text{ M Na}_2\text{SO}_4$

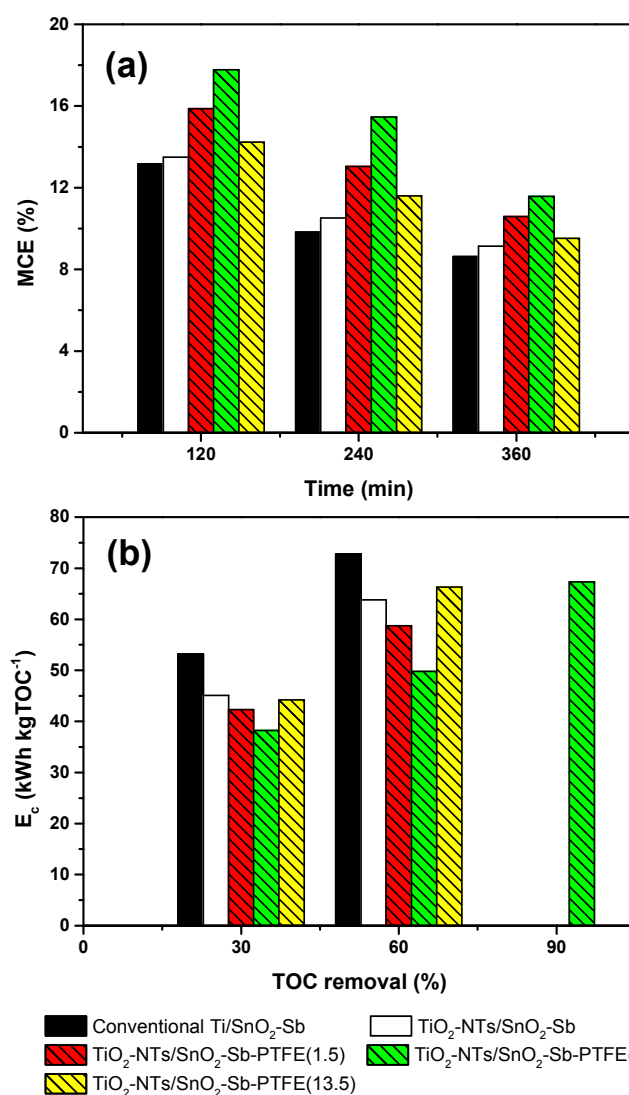
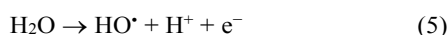


**Fig. 9** (a) MCE changes with time and (b) specific energy consumption with TOC removal rate at pH 7 in  $0.05 \text{ M Na}_2\text{SO}_4$

**3.2.2 Influence of pH.** The effect of pH on phenol oxidation by the different electrodes was investigated in 0.05 M Na<sub>2</sub>SO<sub>4</sub>. Fig. 7 shows that all of the 3 electrodes achieve better TOC removals in acidic solutions than that in neutral and basic solutions. The TOC removals at pH 3 are 74%, 79% and 94% respectively using Ti/SnO<sub>2</sub>-Sb, TiO<sub>2</sub>-NTs/SnO<sub>2</sub>-Sb and TiO<sub>2</sub>-NTs/SnO<sub>2</sub>-Sb-PTFE(4.5) as anodes. The SUVA<sub>254</sub> also decreases more rapidly, indicating a faster ring cleavage of the aromatic intermediates. On the contrary, TOC removals are not favorable at pH 11. The results can be explained from the viewpoint of thermodynamics, because the oxidative power of HO• varies with pH. HO• radicals are generated from the oxidation of water:



Given that the redox potential of HO•<sub>aq</sub>/H<sub>2</sub>O is 2.59 V at pH 0 at the standard condition, the relationship between solution pH and redox potential of HO•<sub>aq</sub>/H<sub>2</sub>O can be calculated by Nernst equation:

$$E^\circ(\text{HO}^\bullet_{\text{aq}}/\text{H}_2\text{O}) = 2.59 - 0.059 \text{ pH} \quad (6)$$

Thus, the values of  $E^\circ(\text{HO}^\bullet_{\text{aq}}/\text{H}_2\text{O})$  are 2.41, 2.18 and 1.94 at pH 3, 7 and 11. Therefore, higher TOC removal can be achieved in low pH range. However, in the basic solution with pH 11, the decrease of TOC removal is at a greater extent using TiO<sub>2</sub>-NTs/SnO<sub>2</sub>-Sb-PTFE(4.5) (82%) as anode than those using conventional Ti/SnO<sub>2</sub>-Sb (64%) and TiO<sub>2</sub>-NTs/SnO<sub>2</sub>-Sb (73%). This is probably because the electrocatalytic oxidation of phenol with TiO<sub>2</sub>-NTs/SnO<sub>2</sub>-Sb-PTFE(4.5) relies more on HO• generation. Hence, the phenol oxidation is greatly influenced when the oxidative power of HO• reduces in the basic solution.

**3.2.3 Influence of supporting electrolytes.** The types of supporting electrolytes may influence the types of oxidative species generated, and hence the process efficiency of electrochemical oxidation. Fig. 10 shows the TOC removals and the corresponding SUVA<sub>254</sub> of phenol using different anodes in 0.05 M Na<sub>2</sub>SO<sub>4</sub> and 0.1 M NaCl at pH 7. TOC removals in the presence of 0.1 M NaCl are slightly higher than those in the presence of 0.05 M Na<sub>2</sub>SO<sub>4</sub> with Ti/SnO<sub>2</sub>-Sb(conventional) and TiO<sub>2</sub>-NTs/SnO<sub>2</sub>-Sb. However, a decrease of TOC removal efficiency is observed with TiO<sub>2</sub>-NTs/SnO<sub>2</sub>-Sb-PTFE(4.5). The reactive chlorine will be generated in the presence of Cl<sup>-</sup> through the following reactions:

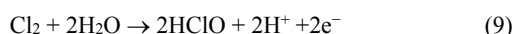
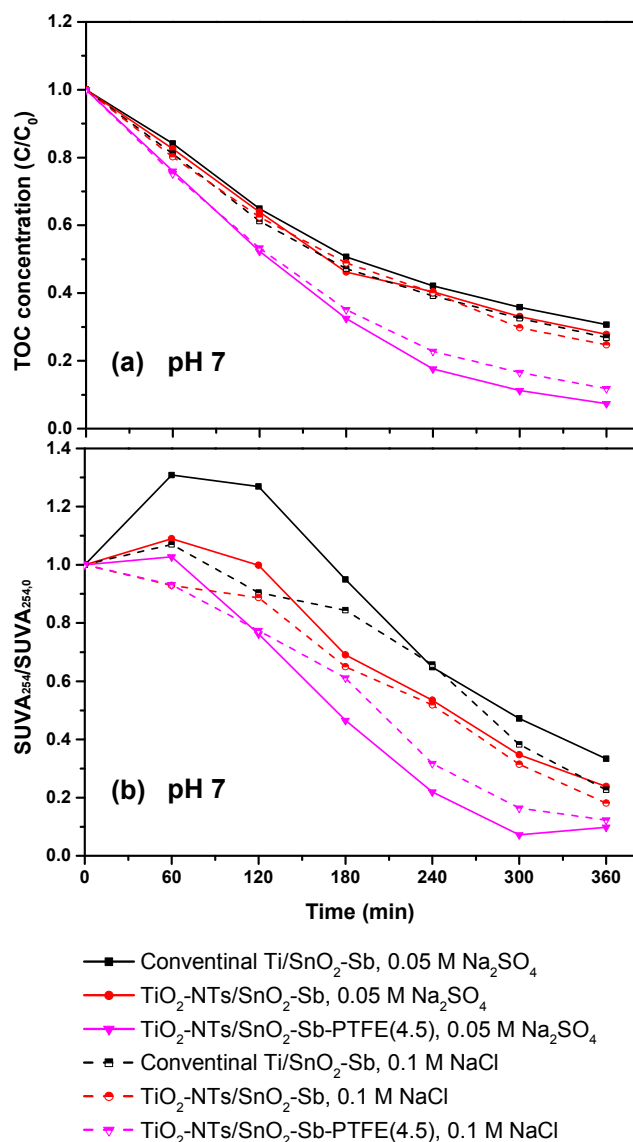
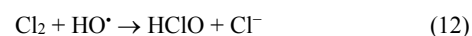
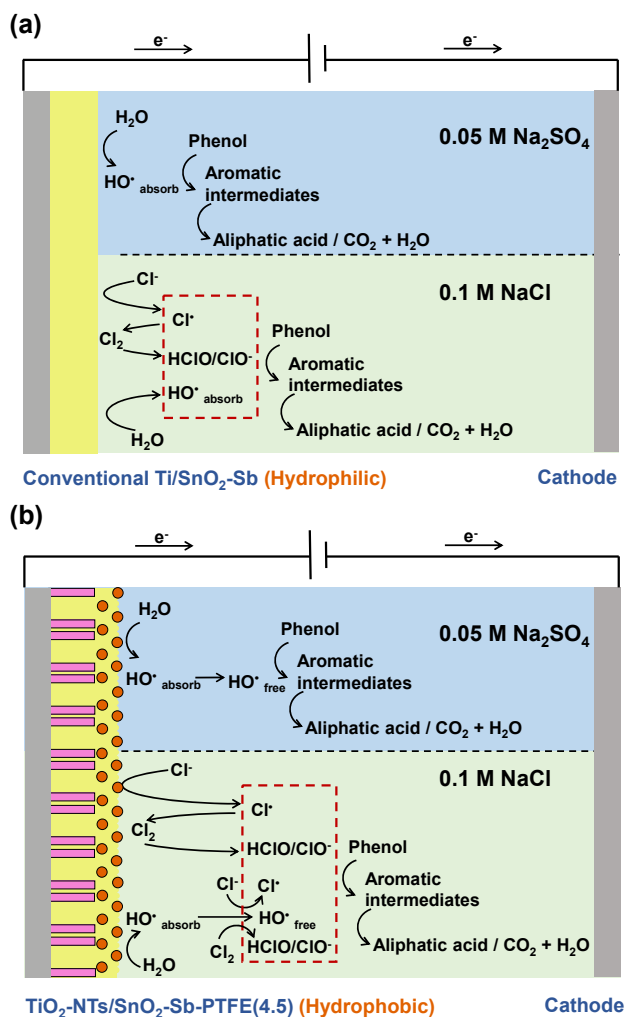


Fig. 11 shows the schematic illustration of electrochemical oxidation of phenol using TiO<sub>2</sub>-NTs/SnO<sub>2</sub>-Sb-PTFE(4.5) and the conventional Ti/SnO<sub>2</sub>-Sb as anodes in 0.05 M Na<sub>2</sub>SO<sub>4</sub> and 0.1 M NaCl. Since Cl<sub>2</sub> can only present in the solution in very low pH (usually < 1), the main reactive chlorine species for phenol oxidation are Cl<sup>•</sup>, HClO and ClO<sup>•</sup>. Although the oxidative power of Cl<sup>•</sup> (2.2 V), HClO (1.63 V) and ClO<sup>•</sup> (0.90 V) are lower than that of HO• (2.59 V), their advantages of massive production and longer lifetime over HO• make them degrade phenol more effectively. However, for TiO<sub>2</sub>-NTs/SnO<sub>2</sub>-Sb-PTFE(4.5) electrode which has superior generation of free HO• due to its hydrophobic surface, the TOC removal of phenol is inhibited by the following competing reactions:<sup>38</sup>



**Fig. 10** TOC concentration and SUVA<sub>254</sub> as a function of time during phenol degradation at: (a) pH 7; (b) pH 3; (c) pH 11

The Cl<sup>•</sup> and Cl<sub>2</sub> played the role of HO• scavengers so that TOC removal by free HO• is not favorable. Therefore, the TOC removal efficiency decreases in 0.1 M NaCl. All of the 3 electrodes obtain faster SUVA<sub>254</sub> decrease in the presence of NaCl in the first 2 h (Fig. 10). This is because reactive chlorine tends to react with electron rich moieties such as of aromatic intermediates,<sup>39</sup> hence, the aromatic rings open more easily. However, after 2 h the decrease of SUVA<sub>254</sub> of phenol with TiO<sub>2</sub>-NTs/SnO<sub>2</sub>-Sb-PTFE(4.5) is slower in 0.1 M NaCl than that in 0.05 M Na<sub>2</sub>SO<sub>4</sub>, indicating the inhibition of phenol degradation by less amount of HO•.



**Fig. 11** Schematic illustration of electrochemical oxidation of phenol in 0.05 M Na<sub>2</sub>SO<sub>4</sub> and 0.1 M NaCl using (a) conventional Ti/SnO<sub>2</sub>-Sb and (b) TiO<sub>2</sub>-NTs/SnO<sub>2</sub>-Sb-PTFE(4.5)

### 3.3 Leaching of Sn ions

In industrial application using SnO<sub>2</sub> electrodes for removing organic compounds, the leaching of Sn ions has become an issue of concern which may cause the secondary pollution. Fig. 12a shows the concentration of Sn ions released from the electrodes after 6 h electrochemical oxidation at different initial solution pH in 0.05 M Na<sub>2</sub>SO<sub>4</sub>. Sn concentrations detected at Ti/SnO<sub>2</sub>-Sb (conventional) were larger than those of TiO<sub>2</sub>-NTs/SnO<sub>2</sub>-Sb and TiO<sub>2</sub>-NTs/SnO<sub>2</sub>-Sb-PTFE electrodes at all solution pH. At pH 3, Sn dissolved concentration was  $1.1 \times 10^{-4}$  M using the conventional Ti/SnO<sub>2</sub>-Sb as anode, while those released from TiO<sub>2</sub>-NTs/SnO<sub>2</sub>-Sb-PTFE electrodes were  $7.1 \times 10^{-5}$  M to  $8.0 \times 10^{-5}$  M. With the increase of initial solution pH from 3 to 7, Sn leaching further decreased but not significantly. However, at initial solution pH 11, only trace amount of Sn ions was detected with the lowest value of  $3.6 \times 10^{-6}$  M at TiO<sub>2</sub>-NTs/SnO<sub>2</sub>-Sb-PTFE(13.5). The concentration of the leached Sn ions was greatly influenced by the final solution pH. During OER at anodes, the simultaneous generation of H<sup>+</sup> gives rise to a dramatic decrease of solution pH. The high OEP of TiO<sub>2</sub>-NTs/SnO<sub>2</sub>-Sb-PTFE electrodes could inhibit the OER, thus less H<sup>+</sup> is generated and Sn leaching is not favorable. Final solution pH was low at initial

solution pH 3 and 7. However, the final solution pH was near neutral at initial solution pH 11, where the dissolution of Sn ions is inhibited. On the other hand, PTFE could also present a barrier for SnO<sub>2</sub> and electrolytes to contact, which inhibits the anodic dissolution of SnO<sub>2</sub>.

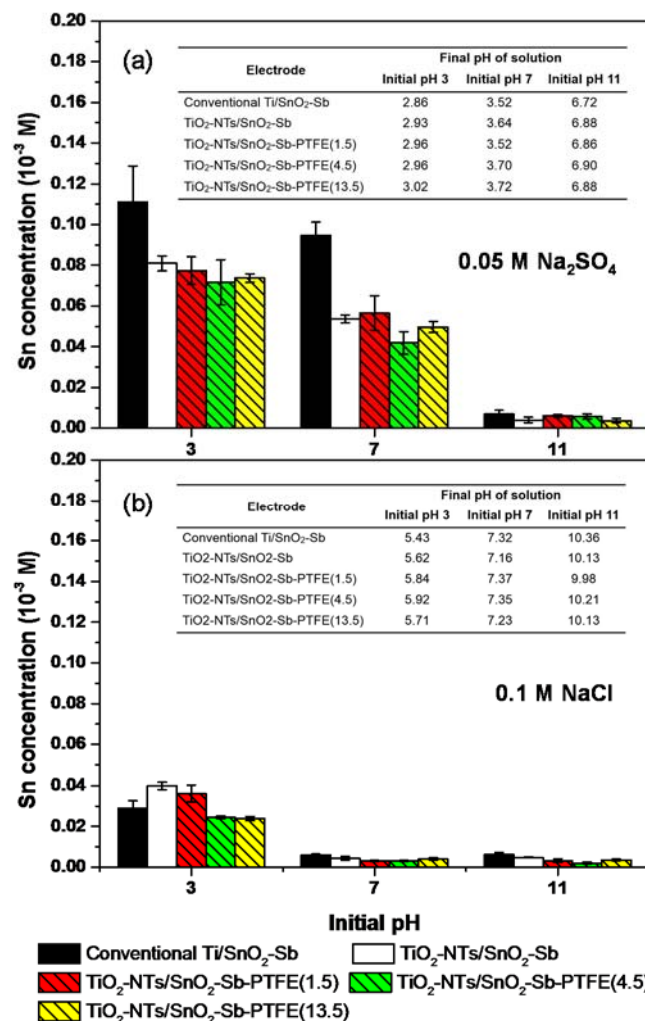


**Fig. 12** Leached Sn ions concentration ( $\pm$  S.D) after 6 h electrochemical oxidation in (a) 0.05 M Na<sub>2</sub>SO<sub>4</sub> and (b) 0.1 M NaCl (insets are the final pH of solutions after 6 h electrochemical oxidation)

The Sn ions leaching can be further inhibited using 0.1 M NaCl as supporting electrolyte (Fig. 12b). Cl<sub>2</sub> can be generated at anode surface without H<sup>+</sup> generation, but the solution H<sup>+</sup> is consumed at the cathode to form H<sub>2</sub>. Thus, there is an increase of solution pH after 6 h of electrochemical oxidation. Therefore, Sn ions are not likely to be leached out. Lowest Sn ions concentration was detected to be only  $2 \times 10^{-6}$  M at basic solution with initial pH 11 using TiO<sub>2</sub>-NTs/SnO<sub>2</sub>-Sb-PTFE(4.5). In general, the TiO<sub>2</sub>-NTs/SnO<sub>2</sub>-Sb-PTFE can effectively inhibit the leaching of Sn ions through the presence of PTFE layer.

### Conclusions

TiO<sub>2</sub>-NTs/SnO<sub>2</sub>-Sb-PTFE composite electrode with high hydrophobic surface, high oxygen evolution potential (2.4 V vs Ag/AgCl), small electrochemical resistance and good stability

was successfully prepared by pulse electrodeposition method. The TiO<sub>2</sub>-NTs/SnO<sub>2</sub>-Sb-PTFE exhibited remarkably better electrocatalytic performance for phenol degradation than the conventional Ti/SnO<sub>2</sub>-Sb prepared by thermochemical decomposition and TiO<sub>2</sub>-NTs/SnO<sub>2</sub>-Sb without PTFE. The TOC removal and SUVA<sub>254</sub> degradation of phenol confirmed 4.5 mL L<sup>-1</sup> to be the optimal PTFE loading for TiO<sub>2</sub>-NTs/SnO<sub>2</sub>-Sb-PTFE electrodes. The pH and types of supporting electrolytes (Na<sub>2</sub>SO<sub>4</sub> and NaCl) had more significant influence on phenol oxidation efficiency with TiO<sub>2</sub>-NTs/SnO<sub>2</sub>-Sb-PTFE(4.5) electrode, which had the superior ability of HO<sup>•</sup> generation because of its hydrophobic surface. The TiO<sub>2</sub>-NTs/SnO<sub>2</sub>-Sb-PTFE also showed leaching-resistant for the leaching of Sn ion, making it have the environmental merit for the degradation of recalcitrant organic pollutants in aquatic systems.

### Acknowledgements

The authors would like to gratefully acknowledge Nanyang Technological University (NTU) for the award of PhD research scholarship. Nanyang Environment and Water Research Institute (NEWRI) and Singapore Institute of Manufacturing Technology (SIMTech) are thanked for the provision of experimental facilities.

### Notes and references

<sup>a</sup> School of Civil and Environmental Engineering, Nanyang Technological University, 50 Nanyang Avenue, Singapore 639798, Singapore. E-mail: [cutlim@ntu.edu.sg](mailto:cutlim@ntu.edu.sg); Tel: +65-6790 6933, Fax: +65-6791 0676

<sup>b</sup> Nanyang Environment & Water Research Institute (NEWRI), Nanyang Technological University, 1 Cleantech Loop, CleanTech One, Singapore 637141, Singapore.

<sup>c</sup> Singapore Institute of Manufacturing Technology, 71 Nanyang Drive, 638075, Singapore.

- G. H. Chen, *Sep. Purif. Technol.*, 2004, **38**, 11-41.
- M. Panizza and G. Cerisola, *Chem. Rev.*, 2009, **109**, 6541-6569.
- J. D. Rodgers, W. Jedral and N. I. Bunce, *Environ. Sci. Technol.*, 1999, **33**, 1453-1457.
- C. A. Martinez-Huitle and S. Ferro, *Chem. Soc. Rev.*, 2006, **35**, 1324-1340.
- G. R. Malpass, D. W. Miwa, S. A. Machado and A. J. Motheo, *J. Hazard. Mater.*, 2010, **180**, 145-151.
- J. M. Aquino, R. C. Rocha-Filho, L. A. M. Ruotolo, N. Bocchi and S. R. Biaggio, *Chem. Eng. J.*, 2014, **251**, 138-145.
- W. Wu, Z.-H. Huang and T.-T. Lim, *Applied Catalysis A: General*, 2014, **480**, 58-78.
- G. R. Malpass, D. W. Miwa, S. A. Machado, P. Olivi and A. J. Motheo, *J. Hazard. Mater.*, 2006, **137**, 565-572.
- L. H. Tran, P. Drogui, G. Mercier and J. F. Blais, *J Environ Eng-Asce*, 2009, **135**, 1051-1062.
- G. H. Zhao, X. Cui, M. C. Liu, P. Q. Li, Y. G. Zhang, T. C. Cao, H. X. Li, Y. Z. Lei, L. Liu and D. M. Li, *Environ. Sci. Technol.*, 2009, **43**, 1480-1486.
- C. Borrás, C. Berzoy, J. Mostany, J. C. Herrera and B. R. Scharifker, *Appl Catal B-Environ*, 2007, **72**, 98-104.
- X. M. Chen, F. R. Gao and G. H. Chen, *J. Appl. Electrochem.*, 2005, **35**, 185-191.
- C. L. P. S. Zanta, P. A. Michaud, C. Comninellis, A. R. De Andrade and J. F. C. Boodts, *J. Appl. Electrochem.*, 2003, **33**, 1211-1215.
- B. CorreaLozano, C. Comninellis and A. DeBattisti, *J. Appl. Electrochem.*, 1997, **27**, 970-974.
- H. Lin, J. Niu, J. Xu, H. Huang, D. Li, Z. Yue and C. Feng, *Environ. Sci. Technol.*, 2013, **47**, 13039-13046.

- H. Lin, J. Niu, J. Xu, Y. Li and Y. Pan, *Electrochim. Acta*, 2013, **97**, 167-174.
- Q. F. Zhuo, S. B. Deng, B. Yang, J. Huang and G. Yu, *Environ. Sci. Technol.*, 2011, **45**, 2973-2979.
- Y. Feng, Y. H. Cui, J. Liu and B. E. Logan, *J. Hazard. Mater.*, 2010, **178**, 29-34.
- Y. J. Feng, Y. H. Cui, B. Logan and Z. Q. Liu, *Chemosphere*, 2008, **70**, 1629-1636.
- G. Li, Y.-H. Wang and Q.-Y. Chen, *J. Solid State Electrochem.*, 2013, **17**, 1303-1309.
- Y. Liu, H. L. Liu, J. Ma and J. J. Li, *J. Hazard. Mater.*, 2012, **213**, 222-229.
- Q. L. Zhang, Y. C. Liu, D. M. Zeng, J. P. Lin and W. Liu, *Water Sci. Technol.*, 2011, **64**, 2023-2028.
- Y. Chu, D. Zhang, L. Liu, Y. Qian and L. Li, *J. Hazard. Mater.*, 2013, **252-253C**, 306-312.
- D. L. He and S. I. Mho, *J. Electroanal. Chem.*, 2004, **568**, 19-27.
- Q. Wang, T. Jin, Z. Hu, L. Zhou and M. Zhou, *Sep. Purif. Technol.*, 2013, **102**, 180-186.
- Y. Chen, L. Hong, H. M. Xue, W. Q. Han, L. J. Wang, X. Y. Sun and J. S. Li, *J. Electroanal. Chem.*, 2010, **648**, 119-127.
- W. Han, C. Zhong, L. Liang, Y. Sun, Y. Guan, L. Wang, X. Sun and J. Li, *Electrochim. Acta*, 2014, **130**, 179-186.
- T. Wu, G. H. Zhao, Y. Z. Lei and P. Q. Li, *J Phys Chem C*, 2011, **115**, 3888-3898.
- B. J. Hwang and K. L. Lee, *J. Appl. Electrochem.*, 1996, **26**, 153-159.
- G. H. Zhao, Y. G. Zhang, Y. Z. Lei, B. Y. Lv, J. X. Gao, Y. A. Zhang and D. M. Li, *Environ. Sci. Technol.*, 2010, **44**, 1754-1759.
- T. G. Duan, Y. Chen, Q. Wen and Y. Duan, *Rsc Adv*, 2014, **4**, 57463-57475.
- F. Montilla, E. Morallon, A. De Battisti and J. L. Vazquez, *J. Phys. Chem. B*, 2004, **108**, 5036-5043.
- C. Tai, J. F. Peng, J. F. Liu, G. B. Jiang and H. Zou, *Anal. Chim. Acta*, 2004, **527**, 73-80.
- L. Liu, G. H. Zhao, M. F. Wu, Y. Z. Lei and R. Geng, *J. Hazard. Mater.*, 2009, **168**, 179-186.
- L. M. Da Silva, L. A. De Faria and J. F. C. Boodts, *J. Electroanal. Chem.*, 2002, **532**, 141-150.
- J. L. Weishaar, G. R. Aiken, B. A. Bergamaschi, M. S. Fram, R. Fujii and K. Mopper, *Environ. Sci. Technol.*, 2003, **37**, 4702-4708.
- M. E. Makgae, M. J. Klink and A. M. Crouch, *Appl Catal B-Environ*, 2008, **84**, 659-666.
- J. E. Grebel, J. J. Pignatello and W. A. Mitch, *Environ. Sci. Technol.*, 2010, **44**, 6822-6828.
- O. Scialdone, S. Randazzo, A. Galia and G. Silvestri, *Water Res.*, 2000, **43**, 2260-2272.

RSC Advances Accepted Manuscript